Acta Cryst. (1978). B34, 1060–1065

Powder Profile Refinement of Lead Zirconate Titanate at Several Temperatures.
I. $PbZr_{0.9}Ti_{0.1}O_3$

By A. M. Glazer and S. A. Mabud*
Clarendon Laboratory, Parks Road, Oxford OX1 3PU, England
and R. Clarke
Cavendish Laboratory, Madingley Road, Cambridge CB3 0HE, England

(*Received* 23 *September* 1977; *accepted* 28 *October* 1977)

The Rietveld neutron powder profile analysis of $PbZr_{0.9}Ti_{0.1}O_3$ is reported at various temperatures. Cation displacements and octahedral distortions are observed to decrease smoothly with increasing temperature, as expected for a ferroelectric. The loss of the octahedron tilt angle is observed at the $F_{R(LT)}$ to $F_{R(HT)}$ transition.

Introduction

In this paper we report the results of neutron powder profile refinement (Rietveld, 1969) on $PbZr_{0.9}Ti_{0.1}O_3$ which is a member of the technologically important PZT series (Fig. 1) and has found application in pyroelectric detectors. As can be seen in Fig. 1 there are two high-temperature phase transitions [$F_{R(LT)}$ to $F_{R(HT)}$ and $F_{R(HT)}$ to cubic] and these can be observed in the temperature dependence of the spontaneous polarization, P_s (Fig. 2*a*). The sharp downward step in P_s, in particular, leads to a large pyroelectric coefficient $p = dP_s/dT$ associated with a small dielectric anomaly (Fig. 2*b*). This combination of properties favours its use in pyroelectric detectors (Clarke & Glazer 1976*a*; Clarke, Glazer, Ainger, Appleby, Poole & Porter, 1976). The three phases of $PbZr_{0.9}Ti_{0.1}O_3$ are summarized in Table 1. At room temperature $F_{R(LT)}$ is rhombohedral with the pseudocubic axes doubled. Here, the Pb and Zr/Ti atoms are displaced parallel to one another along [111] to give a polar ferroelectric phase. In addition, the O octahedra are tilted *about* [111] with the tilt system $a^-a^-a^-$, in the notation of Glazer (1972, 1975), to give rise to a doubled unit cell. This structure was originally determined at room temperature by Michel, Moreau, Achenbach, Gerson & James (1969) with modest precision. No study has been made at higher temperatures, although the structure of $F_{R(HT)}$ can be inferred from the work of these authors on $PbZr_{0.58}Ti_{0.42}O_3$. At 100°C these tilts are lost but the cation shifts are retained. Thus $F_{R(HT)}$ is still polar in this phase. Finally, at 250°C the cation displacements are lost to form the paraelectric, cubic phase.

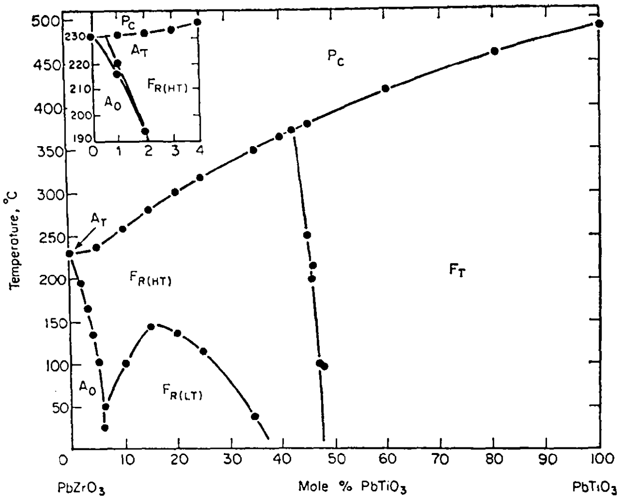

Fig. 1. The phase diagram of the lead zirconate titanate (PZT) system (after Jaffe, Cook & Jaffe, 1971).

To study the structure of $PbZr_{0.9}Ti_{0.1}O_3$ we decided to use the neutron powder method. Although single crystals have been grown (Clarke & Glazer, 1974, 1976*b*; Clarke, Whatmore & Glazer, 1976; Clarke & Whatmore, 1976), they are always twinned and unsuitable for structure determination. The powder technique is rapid and capable of locating the O atom positions precisely. In this paper we show how the positions vary with temperature and their relationship to the spontaneous polarization.

Sample preparation

To make a polycrystalline sample with an appropriate grain size (~10 μm) PbO (99·999% purity; Koch-Light), ZrO_2 (99·8% purity; Koch-Light) and TiO_2 (99·5% purity; Koch-Light) were mixed in the correct

---

* On leave from Cavendish Laboratory, Cambridge.

proportions to form $PbZr_{0\cdot 9}Ti_{0\cdot 1}O_3$ and ground by hand in an agate mortar. Good mixing was checked periodically with a high-power microscope and was achieved in about 1 h. The powder was then cold-pressed into discs, calcined at 500 °C for 2 h in an atmosphere of PbO vapour and air, and subsequently crushed, ground and re-pressed into discs. These were again fired, this time at 800 °C for 2 h. After further crushing, grinding and re-pressing, firing was repeated at 1200 °C for 2 h. Finally the samples were crushed and ground. Throughout this procedure Debye–Scherrer and Guinier–de Wolff photographs were taken with Cu *Kα* radiation in order to monitor the progress of the reaction. The resulting powder closely resembled ceramics made by the Allen Clark Research Laboratories (Plessey Ltd) by chemical coprecipitation techniques and showed a sharp diffraction pattern up to high angles with no sign of any impurity lines. When we were satisfied with the product, about 25 g were sealed under vacuum in a silica tube 5 × 1 × 1 cm.

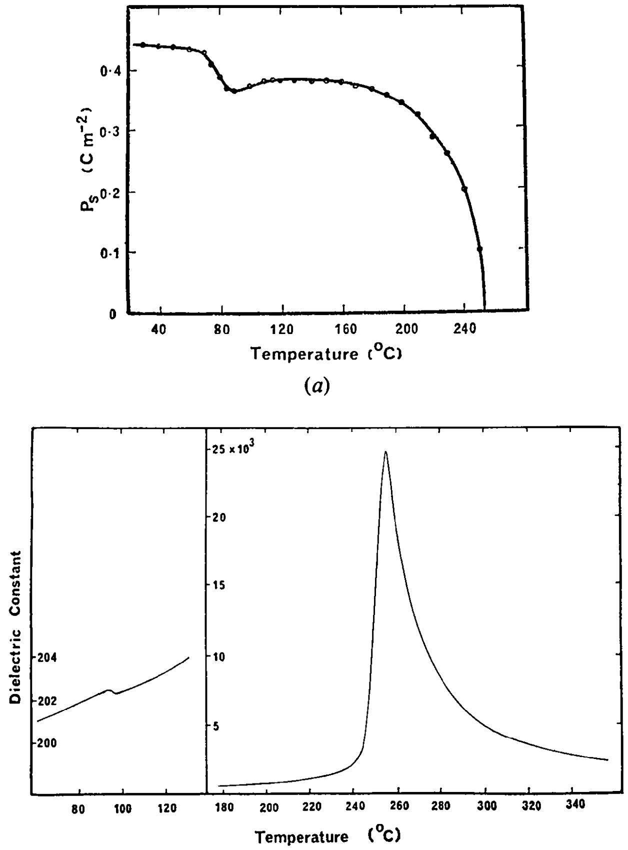

Fig. 2. (*a*) The spontaneous polarization, P_s, of a single crystal of $PbZr_{0\cdot 9}Ti_{0\cdot 1}O_3$ as a function of temperature measured from hysteresis loops at 50 Hz. (*b*) The dielectric constant of $PbZr_{0\cdot 9}Ti_{0\cdot 1}O_3$ as a function of temperature measured at 1·5 kHz. Both transitions can be seen.

Table 1. *Summary of the three phases of* $PbZr_{0\cdot 9}Ti_{0\cdot 1}O_3$

Phase	$F_{R(LT)}$	$F_{R(HT)}$	P_c
Space group	*R3c*	*R3m*	*Pm3m*
Cell geometry	$2a_p \times 2b_p \times 2c_p$	$a_p \times b_p \times c_p$	$a_p \times b_p \times c_p$
Pb displacements	[111]	[111]	–
Zr/Ti displacements	[111]	[111]	–
Oxygen octahedron tilt system (Glazer, 1972)	$a^-a^-a^-$	$a^0a^0a^0$	$a^0a^0a^0$

Data collection, reduction and refinement

Sets of intensities were collected on the PANDA diffractometer on the PLUTO reactor at AERE (Harwell) at 25, 60, 100, 150, 200, 235 and 300 °C (all ± 5 °C); the wavelength used was around 1·32 Å. In each set intensities up to $2\theta \simeq 105°$ were measured, each run taking 24 h to complete. A blank run with the furnace and empty silica tube was also carried out to allow correction for background scattering. Throughout, a bank of nine counters arranged as in Fig. 3 was used, moving through steps of 0·1°; because of the way the counters were wired together, six independent channels of results were obtained, as indicated. In order to have the best signal/noise ratio we combined all six channels by computer in the following way: (*a*) The background due to the furnace and silica tube was subtracted from the measured intensities so that the six resulting channels of intensities came solely from the $PbZr_{0\cdot 9}Ti_{0\cdot 1}O_3$ sample. (*b*) The three in-plane channels, coming from counters constructed with an angular displacement of 5° between them, were added together, allowing for the angular differences by adding or subtracting 5° from the appropriate channels. The same was done for the three out-of-plane channels. (*c*) The two resultant channels were slightly out of phase with respect to each other by differing amounts depending on the angle of diffraction. Within the resolution of the diffractometer it was found that the data could be roughly divided into two regimes: at low angles, the peak positions measured by the in-plane and out-of-plane counters differed by a small but effectively constant positive angle, whereas at higher angles the peaks from both types of counter coincided. In order to make the positions of the low-angle peaks coincide, we chose a region of background intensity between the two regimes and deleted one or two lines of computer data, as necessary, from the out-of-plane set. No correction was made for the insignificant difference in Lorentz factor between in-plane and out-of-plane counters. In this manner a single channel of results was obtained with approximately six times the number of counts from a single counter.

Refinement was carried out with the Rietveld program modified by Hewat (Harwell Report RRL 73/897) with the following scattering lengths: Pb 0·940, Zr/Ti 0·609, O 0·580 × 10^{-12} cm. The variables were: an overall scale factor, three half-width parameters defining the Gaussian line shapes, the counter-zero error, the atomic position parameters, isotropic or anisotropic temperature factors, and unit-cell parameters defined in the following paragraph. Occasionally the preferred orientation and asymmetry parameters were refined as well, but their effects were never significant. As a check, the scattering lengths were also refined but their final values never differed significantly from the initial ones.

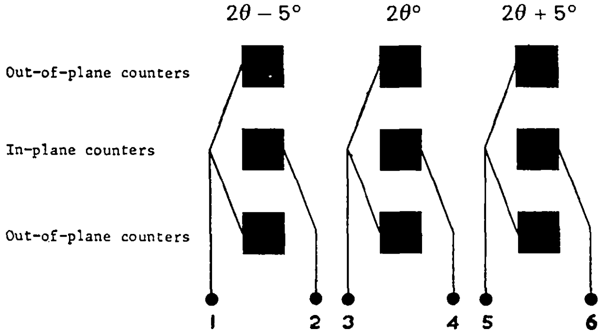

Fig. 3. Schematic diagram of the bank of counters used in PANDA. The nine counters are connected as shown to produce six channels.

In order to have structural parameters which were simple to visualize we chose, in the rhombohedral phases, to use hexagonal axes, a_h, b_h and c_h, specified with respect to the double pseudocubic cell $2a_p \times 2b_p \times 2c_p$ by the matrix

$$\begin{pmatrix} \frac{1}{2} & 0 & \frac{\bar{1}}{2} \\ \frac{\bar{1}}{2} & \frac{1}{2} & 0 \\ 1 & 1 & 1 \end{pmatrix}$$

As has been described by Megaw & Darlington (1975), the fractional position parameters of the $R3c$ phase $[F_{R(\mathrm{LT})}]$ with a hexagonal cell of height $c_h \simeq 14$ Å are given by

	x	y	z
Pb	0	0	$\frac{1}{4}+s$
Zr/Ti	0	0	t
O	$\frac{1}{6}-2e-2d$	$\frac{1}{3}-4d$	$\frac{1}{12}$

where s and t measure the fractional cation displacements along the threefold axis with respect to an origin chosen to lie midway between opposite faces of an O octahedron. Parameter d describes the way an octahedron is distorted, keeping triad-axis symmetry, but making the upper and lower faces different in size. Parameter e indicates the rotation of an octahedron about the triad axis with the angle of tilt, ω, given by $\tan\omega = 4\sqrt{3}e$. In the $R3m$ $[F_{R(\mathrm{HT})}]$ phase there are no

Table 2. *Refined position parameters*

	Literature results*	25°C	60°C	100°C	150°C	200°C	235°C	300°C
Phase		$F_{R(\mathrm{LT})}$		$F_{R(\mathrm{HT})}$				P_c
Space group		$R3c$ (C_{3v}^6)		$R3m$ (C_{3v}^5)				$Pm3m$ (O_h^1)
a_h (Å)		5·8412	5·8434	5·8479	5·8510	5·8543	5·8564	–
c_h (Å)		14·4122	14·4178	14·4239	14·4222	14·4115	14·3951	–
a_p (Å)		4·1404	4·1420	4·1447	4·1460	4·1465	4·1459	4·1449
α(°)		89·722	89·722	89·735	89·760	89·810	89·867	90·000
s	0·022 (2)	0·0316 (8)	0·0307 (8)	0·0266 (11)	0·0257 (12)	0·0183 (11)	0·0146 (29)	–
t	0·006 (2)	0·0114 (11)	0·0112 (10)	0·0095 (16)	0·0077 (16)	0·0072 (13)	0·0021 (47)	–
d	?	−0·0029 (3)	−0·0023 (3)	−0·0021 (4)	−0·0011 (11)	−0·0009 (4)	−0·0007 (9)	–
e	0·019 (2)	0·0137 (5)	0·0122 (6)	–	–	–	–	–
ω (°)	7·5 (6)	5·42 (20)	4·83 (24)	–	–	–	–	–
Number of parameters		25	25	22	22	22	22	12
Number of reflections		80	85	56	59	50	59	21
R_{nuc} (%)		6·33	6·21	5·91	7·06	6·25	5·00	5·68
R_{prof} (%)		11·75	13·93	13·26	17·15	13·26	16·28	15·51
R_{exp} (%)		5·06	6·18	5·70	9·60	4·86	6·08	4·71
Number of counts in pseudocubic 200 reflection		17 900	26 000	25 900	10 000†	30 300	25 400	33 700

$R_{\mathrm{nuc}} = 100\,\Sigma\,|I(\mathrm{obs.}) - I(\mathrm{calc.})|/\Sigma\,I(\mathrm{obs.})$
$R_{\mathrm{prof}} = 100\,\Sigma\,|y(\mathrm{obs.}) - y(\mathrm{calc.})|/\Sigma\,|y\,(\mathrm{obs.})|$
$R_{\mathrm{exp}} = 100\,\sqrt{[(N-P)/\Sigma\,wy(\mathrm{obs.})^2]}$
I(obs.), I(calc.) = observed and calculated integrated intensity of each reflection
y(obs.), y(calc.) = observed and calculated profile data point
w = weight allotted to each data point

* From Michel *et al.* (1969) at room temperature.

† The low count with this run was because the measurements were carried out near the end of the reactor cycle and when the monitor count rate was at its lowest.

tilts and therefore e is set to zero. As the pseudocubic cell is not doubled in this phase the simplest (and conventional) hexagonal cell has half the height of the $R3c$ cell. However, in order to compare the two phases it is easiest if everything is referred to a doubled hexagonal cell with $c_h \simeq 14$ Å. To accomplish this for $R3m$ we used the same symmetry operators as for $R3c$ but added the constraint that for the prototype O atom, $2x = y$. The effect of this constraint is to introduce, artificially into the unit cell, mirror planes containing the threefold axis and each O atom.

After preliminary refinement to establish the scale factor and the half-width parameters, several cycles were carried out refining position parameters and isotropic temperature factors.

It was always found that the refinement did not proceed quite as would normally be expected in the rhombohedral phases. General experience with Rietveld refinement of simple perovskites has shown that it is possible to refine to a very low nuclear R factor (R_{nuc}) (defined in Table 2), usually around 2–3% (Hewat, 1973). In our case R_{nuc} lay in the range 9–13% and after several cycles the profile R factor, R_{prof}, was typically ~17%. More importantly, the values obtained for the position parameters when refined with the isotropic temperature factors did not seem to us to be very realistic. For example, the displacement, t, of the Zr/Ti atom did not show any well defined change with temperature; one would expect it to decrease in much the same way as the spontaneous polarization (Abrahams, Kurtz & Jamieson, 1968). Every attempt with different starting models always produced the same unrealistic result.

It was therefore decided that anisotropic temperature factors should be refined, despite the fact that the Rietveld method is notoriously unreliable at obtaining accurate results for such factors. Refinement this time was much more satisfactory with respect to position parameters, which were quite different from the previous results and which certainly seemed more realistic. Table 2 summarizes the position parameters obtained in this way and Table 3 the anisotropic temperature factors.

Fig. 4 shows calculated and observed intensity profiles for the three phases. Note the disappearance in $F_{R(\text{HT})}$ of the difference reflections (arrowed) caused by octahedral tilting. There is very little apparent difference between the profiles in the $F_{R(\text{HT})}$ and cubic phases. The fit between observed and calculated profiles is quite good. Table 2 shows that R_{nuc} is now considerably lower than before and is roughly the same as the R factor expected on statistical grounds (R_{exp}). Table 2 shows some general trends in the structural parameters. Consider first the s and t parameters plotted in Fig. 5, which can both be seen to fall with increasing temperature; the variation of t in particular is reminiscent of the temperature variation of P_s (Fig. 1), although the standard deviations are large, particularly for high temperatures.

If we relate the spontaneous polarization to the Zr/Ti displacement by $P_s = kt$, the constant k is $2{\cdot}90 \pm 0{\cdot}04$ C m^{-2} Å^{-1}, close to the value $2{\cdot}58$ C m^{-2} Å^{-1} obtained by Abrahams, Kurtz & Jamieson (1968) after averaging over several different materials. There is no reason why one should expect to find such a simple relationship between P_s and t when comparing different materials (Megaw & Darlington, 1975); our result obtained from a single material at different temperatures is probably a more reliable measure of this relationship. It is also clear from Table 2 and Fig. 5 that there is no linear relationship between s and t. This is in contradiction to the assertion of Michel, Moreau, Achenbach, Gerson & James (1969) but in agreement with the findings of Megaw & Darlington. The magnitudes of the position parameters found here differ considerably from those obtained by Michel *et al.* However, this discrepancy should be regarded with caution because during the refinement we always found

Table 3. *Anisotropic temperature factors defined by*
$$\exp[-\tfrac{1}{4}(B_{11}h^2a^{*2} + B_{22}k^2b^{*2} + B_{33}l^2c^{*2} + 2B_{12}hka^*b^* + 2B_{13}hla^*c^* + 2B_{23}klb^*c^*)]$$

		25°C	60°C	100°C	150°C	200°C	235°C	300°C†
Pb	B_{11}	2·45 (18)	2·67 (21)	3·14 (25)	3·95 (30)	4·56 (52)	4·69 (54)	4·73 (18)
	B_{33}	0·53 (40)	0·76 (36)	1·47 (60)	0·09 (52)	2·83 (14)	1·51 (74)	B_{11}
Zr/Ti	B_{11}	0·01 (20)	0·54 (23)	1·21 (24)	1·60 (33)	2·87 (59)	0·37 (48)	0·93 (14)
	B_{33}	2·33 (59)	0·82 (60)	0·18 (49)	−0·09 (66)	−2·77 (68)	1·22 (1·39)	B_{11}
O	B_{11}	1·92 (36)	2·34 (33)	3·70 (31)	4·43 (46)	4·36 (64)	3·28 (62)	1·14 (21)
	B_{22}	0·47 (22)	0·69 (25)	1·83 (32)	1·50 (47)	1·95 (72)	2·36 (1·06)	B_{11}
	B_{33}	1·01 (51)	0·94 (37)	1·64 (50)	4·38 (92)	0·73 (1·31)	3·88 (1·47)	8·42
	B_{12}	0·06 (36)	−0·29 (40)	$\frac{1}{2}B_{22}$	$\frac{1}{2}B_{22}$	$\frac{1}{2}B_{22}$	$\frac{1}{2}B_{22}$	0
	B_{13}	−0·18 (45)	−0·92 (41)	$\frac{1}{2}B_{23}$	$\frac{1}{2}B_{23}$	$\frac{1}{2}B_{23}$	$\frac{1}{2}B_{23}$	0
	B_{23}	−0·67 (18)	−0·87 (19)	−1·07 (24)	−1·81 (42)	−1·42 (53)	−2·09 (77)	0

† Specified relative to the cube axes.

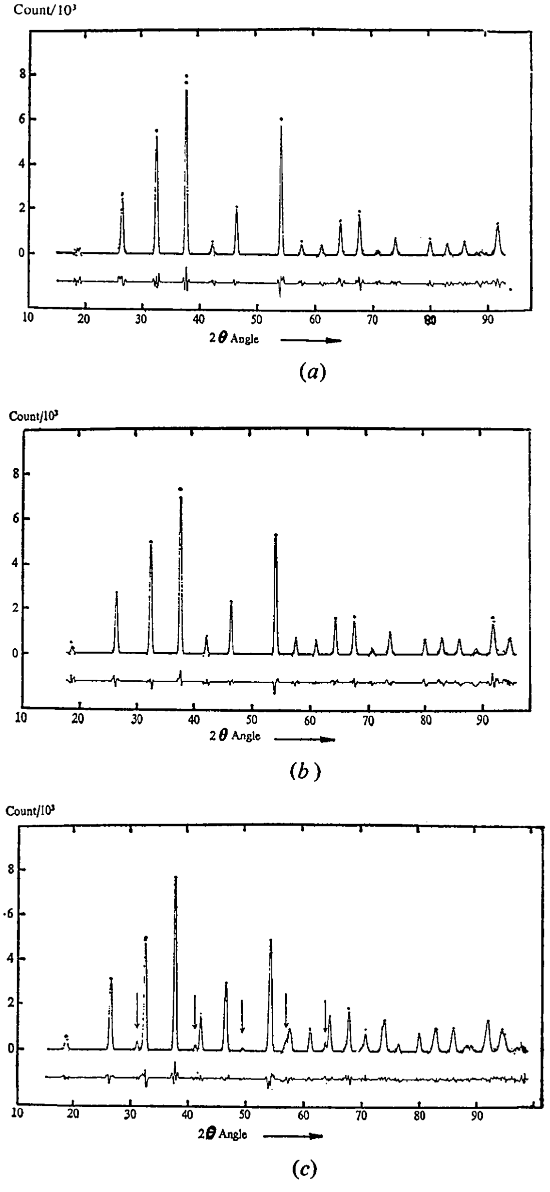

Fig. 4. Observed (dots) and calculated (full line) neutron intensity profiles for the three phases of $PbZr_{0\cdot9}Ti_{0\cdot1}O_3$. The lower trace in each case is the difference between observed and calculated profiles. (*a*) Cubic phase at 300 °C. (*b*) $F_{R(HT)}$ at 200 °C. (*c*) $F_{R(LT)}$ at 25 °C.

that the *s* and *t* parameters were highly correlated. This kind of correlation is typical of the Rietveld analysis technique and cannot as yet be obviated. Despite this, however, there is no reason to expect the ratio *s*/*t* to be incorrect, and, indeed, our room-temperature ratio is similar to the literature value of 3·2.

There is also a large discrepancy between our measurement of the room-temperature tilt angle and that of Michel *et al.* Here, correlation did not affect the issue and we believe our value to be more accurate. It can be seen from Table 2 that the tilt angle decreases at 60 °C, finally becoming zero somewhere near 100 °C. This is shown by the disappearance of the difference reflections (arrowed) in Fig. 4.

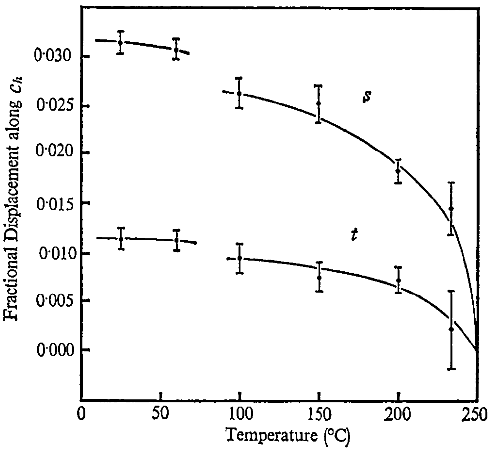

Fig. 5. The variation of cation displacements, *s* and *t*, with temperature.

It can also be seen from Table 2 that the distortion, *d*, of the O octahedron also decreases with increasing temperature. This is to be expected on the general grounds that most departures from the ideal structure decrease with increasing temperature. If we think of the cation displacements, *s* and *t*, as being vertically upwards, the negative sign of *d* implies that the upper face of the octahedron is larger than the lower one. (The lower face is that approached by the displaced Pb atom.) Empirically, one might expect some correlation between *d* and the cation displacements. The present results, however, are not sufficiently precise to enable this correlation to be measured quantitatively, although if one ignores the standard deviations it is found that *d* is roughly proportional to t^2.

The temperature factors in Table 3, although showing large errors, sometimes with negative values for the diagonal terms, do show a surprising consistency between each data set. We always find, for example, that the thermal ellipsoid for the Pb atom appears to be flattened along the threefold axis. The orientations of the O thermal ellipsoids hardly appear to change with temperature and diagonalization of the B_{ij} matrix shows that there is always a large apparent thermal motion, directed along the a_h axis for the prototype O atom. This could possibly correspond to a large tilting motion of the octahedra about [111] of the primitive rhombohedron. However, these values for the B_{ij} are so untrustworthy as to make suspect any attempt at interpretation of them in terms of thermal vibration. Their extreme anisotropy may suggest the possibility of statistical disorder. Nevertheless, we can say that with anisotropic temperature factor refinement we do obtain results for the position parameters which seem to make sense. However, the standard deviations of the position parameters are still larger than are normally encountered (Hewat, 1973, 1974) in simple perovskites. Moreover, the R-factor results are not as good as expected, even in the cubic phase where the only structural parameters to refine are B(Pb), B(Zr/Ti) and B_{11} and B_{22} for oxygen.

We thank the Wolfson Foundation for funds supporting this work and AERE (Harwell) and the SRC for facilities on the PANDA diffractometer.

One of us (SAM) acknowledges a grant from the Commonwealth Scholarship Commission in the United Kingdom.

References

ABRAHAMS, S. C., KURTZ, S. K. & JAMIESON, P. B. (1968). *Phys. Rev.* **172**, 551–553.

CLARKE, R. & GLAZER, A. M. (1974). *J. Phys. C*, **7**, 2147–2156.

CLARKE, R. & GLAZER, A. M. (1976*a*). *Ferroelectrics*, **14**, 695–697.

CLARKE, R. & GLAZER, A. M. (1976*b*). *Ferroelectrics*, **12**, 207–209.

CLARKE, R., GLAZER, A. M., AINGER, F. W., APPLEBY, D., POOLE, N. J. & PORTER, S. G. (1976). *Ferroelectrics*, **11**, 359–364.

CLARKE, R. & WHATMORE, R. (1976). *J. Cryst. Growth*, **33**, 29–38.

CLARKE, R., WHATMORE, R. & GLAZER, A. M. (1976). *Ferroelectrics*, **13**, 497–500.

GLAZER, A. M. (1972). *Acta Cryst.* B**28**, 3384–3392.

GLAZER, A. M. (1975). *Acta Cryst.* A**31**, 756–762.

HEWAT, A. W. (1973). *J. Phys. C*, **6**, 2559–2572.

HEWAT, A. W. (1974). *Ferroelectrics*, **6**, 215–218.

JAFFE, B., COOK, W. R. & JAFFE, H. (1971). *Piezoelectric Ceramics*. London: Academic Press.

MEGAW, H. D. & DARLINGTON, C. N. W. (1975). *Acta Cryst.* A**31**, 161–173.

MICHEL, C., MOREAU, J. M., ACHENBACH, G. D., GERSON, R. & JAMES, W. J. (1969). *Solid State Commun.* **1**, 865–868.

RIETVELD, H. M. (1969). *J. Appl. Cryst.* **2**, 65–71.

Acta Cryst. (1978). B**34**, 1065–1070

Powder Profile Refinement of Lead Zirconate Titanate at Several Temperatures. II. Pure $PbTiO_3$

BY A. M. GLAZER AND S. A. MABUD*

Clarendon Laboratory, Parks Road, Oxford OX1 3PU, England

(*Received* 23 *September* 1977; *accepted* 28 *October* 1977)

The structure of pure $PbTiO_3$ has been refined at −183, −115, 25 and 550°C by the Rietveld neutron powder profile method. Positional parameters and temperature factors are given. No evidence was found for the previously reported low-temperature phase transitions.

Introduction

The perovskite $PbTiO_3$ is of interest for several reasons. At room temperature it shows a somewhat higher tetragonal distortion than $BaTiO_3$, with the cation displacements in its polar phase markedly larger. $PbTiO_3$ remains a tetragonal ferroelectric over a wide range of temperature, in contrast to $BaTiO_3$ and similar materials. The ferroelectric-to-paraelectric transition temperature in $PbTiO_3$ is also higher than in any other material possessing the same structure. Moreover, it is regarded as providing an example of a truly classical ferroelectric phase transition (Shirane, Axe, Harada & Remeika, 1970; Burns & Scott, 1973) with a well defined underdamped soft mode.

Industrially, $PbTiO_3$ is an important material because of its potentially high spontaneous polarization (although when pure it appears to have a high conductivity) and because its solid solutions with $PbZrO_3$ (PZT), $BaTiO_3$, $SrTiO_3$ *etc.*, form ceramics with possible technological applications, such as electromechanical transducers, dielectric devices and pyroelectric detectors.

We have grown high-quality single crystals of a suitable size for X-ray and dielectric experiments with a PbO flux. However, crystals large enough for neutron

---

* On leave from Cavendish Laboratory, Cambridge.